

# A Codeposition Route to CuI–Pyridine Coordination Complexes for Organic Light-Emitting Diodes

Zhiwei Liu,<sup>†</sup> Munzarin F. Qayyum,<sup>‡</sup> Chao Wu,<sup>†</sup> Matthew T. Whited,<sup>†</sup> Peter I. Djurovich,<sup>†</sup> Keith O. Hodgson,<sup>‡,§</sup> Britt Hedman,<sup>§</sup> Edward I. Solomon,<sup>‡</sup> and Mark E. Thompson<sup>\*,†</sup>

<sup>†</sup>Department of Chemistry, University of Southern California, Los Angeles, California 90089, United States

<sup>‡</sup>Department of Chemistry, Stanford University, Stanford, California 94305, United States

<sup>§</sup>Stanford Synchrotron Radiation Lightsource, SLAC, Stanford University, Stanford, California 94309, United States

**S** Supporting Information

**ABSTRACT:** We demonstrate a new approach for utilizing CuI coordination complexes as emissive layers in organic light-emitting diodes that involves in situ codeposition of CuI and 3,5-bis(carbazol-9-yl)pyridine (mCPy). With a simple three-layer device structure, pure green electroluminescence at 530 nm from a Cu(I) complex was observed. A maximum luminance and external quantum efficiency (EQE) of 9700 cd/m<sup>2</sup> and 4.4%, respectively, were achieved. The luminescent species was identified as [CuI(mCPy)<sub>2</sub>]<sub>2</sub> on the basis of photophysical studies of model complexes and X-ray absorption spectroscopy.

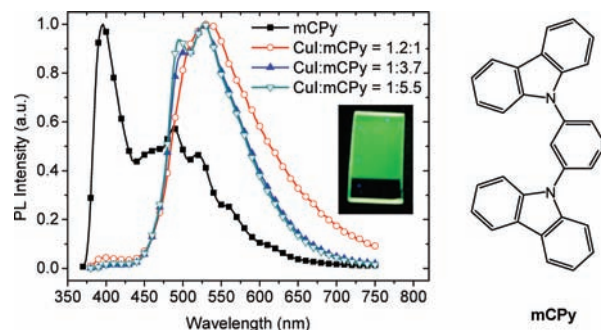


**Figure 1.** (left) PL spectra ( $\lambda_{\text{ex}} = 350$  nm) of a neat mCPy film at 77 K and CuI:mCPy films at rt. Inset: photo of a CuI:mCPy film under UV light (365 nm). (right) Chemical structure of mCPy.

Tremendous improvements in organic light-emitting diodes (OLEDs) have been achieved using phosphorescent emissive Ir-based complexes.<sup>1</sup> Unfortunately, Ir is low in natural abundance, so there has been an increasing interest in luminescent Cu(I) complexes<sup>2</sup> for use in high-efficiency OLEDs. However, since most Cu(I) complexes are unstable toward sublimation<sup>3</sup> and hence not amenable to the vacuum deposition methods typically used to fabricate OLEDs, few devices containing such emitters have been reported.<sup>4</sup>

Among luminescent Cu(I) complexes, those based on CuI are well-known for their structural diversity, rich photophysical behavior, and high luminance efficiency.<sup>5</sup> A wide range of structure motifs have been prepared by combining CuI and pyridine-based ligands in different ratios.<sup>6</sup> Excited states in the resulting complexes have been proposed to be halide-to-ligand charge transfer (XLCT), metal-to-ligand charge transfer (MLCT), and/or halide-to-metal charge transfer (XMCT) states on the basis of experimental and computational studies.<sup>5a,7</sup> Generally, CuI-based complexes, especially with pyridine-based ligands, are highly emissive at room temperature (rt) regardless of the structure and nature of the excited state. However, the application of these complexes in OLEDs has not been demonstrated because of the aforementioned difficulties with sublimation and their poor solubility or stability in solution. In this paper, we demonstrate that codeposition of CuI and 3,5-bis(carbazol-9-yl)pyridine (mCPy; Figure 1) is an efficient way to utilize CuI complexes as emissive materials in OLEDs. Devices made using CuI:mCPy films exhibit pure green electroluminescence (EL) from a Cu(I) emitting species. The chemical composition of the

luminescent species in the codeposited film has been deduced through studies of model complexes and X-ray absorption spectroscopy (XAS) and determined to be primarily [CuI(mCPy)<sub>2</sub>]<sub>2</sub>.

Figure 1 shows the photoluminescence (PL) spectra of a series of CuI:mCPy films made by codepositing CuI and mCPy in different molar ratios from two separate heating sources in a vacuum chamber. For comparison, the PL spectrum of a neat mCPy film at 77 K is also shown in Figure 1. The spectrum for the neat mCPy film consists of an overlapping fluorescence band at 400 nm [biexponential decay,  $\tau = 10.9$  (17%) and 2.0 (83%) ns] and a phosphorescence band at 500 nm (monoexponential decay,  $\tau = 0.48$  s). PL was observed for codeposited CuI:mCPy films over a wide range of molar ratios, with quantum yields as high as 64%. The PL spectra from CuI:mCPy films are dominated by a band centered near 520 nm and have decay lifetimes (Table 1) that differ markedly from that of the mCPy film, implying the formation of phosphorescent Cu(I) complexes. The emission spectra of CuI:mCPy films sometimes show an additional feature at 495 nm (Figure 1). While the shoulder at 495 nm is coincident with the phosphorescence band of neat mCPy, other data are inconsistent with emission from the neat ligand. Transient measurements at the two wavelengths gave the same biexponential lifetimes listed in Table 1 for each composition. In addition, the CuI:mCPy film had identical PL spectra at 298 and 77 K. If the band at 495 nm were caused by emission

**Received:** July 23, 2010

**Published:** March 02, 2011

Table 1. Photophysical Data for Codeposited Films

CuI:mCPy molar ratio	$\lambda_{em}$ (nm)	PLQY (%) <sup>a</sup>	lifetime ( $\mu$ s) <sup>b</sup> [percentage (%)]
1.8:1.0	—	0	—
1.2:1.0	532	8	0.5 [32], 3.0 [68]
1.0:2.3	496, 528	48	3.1 [28], 10.1 [72]
1.0:2.6	502, 528	62	4.4 [35], 12.8 [65]
1.0:3.7	500, 528	63	3.4 [21], 11.5 [79]
1.0:5.5	495, 528	64	3.5 [28], 11.6 [72]

<sup>a</sup> PL quantum yield. <sup>b</sup> Emission lifetimes were measured at 520 nm with excitation wavelength of 331 nm.

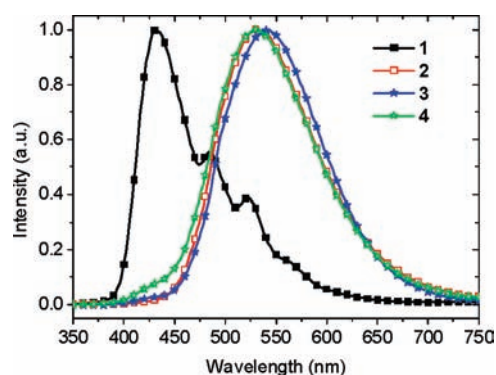


Figure 2. EL spectra of ITO/NPD/EML/BCP/LiF/Al devices at 8 V, where EML denotes neat mCPy (device 1), 1:4 CuI:mCPy (device 2), 1:6 CuI:mCPy (device 3), or 1:10 CuI:mCPy (device 4).

from neat mCPy, one would expect it to be more prominent at lower  $T$ . Thus, the 495 nm feature is likely due to a second Cu(I) complex at low concentration.

To verify that CuI:mCPy complexes are responsible for the luminescence from codeposited films, we prepared a film by codepositing CuI and 1,3-bis(carbazol-9-yl)benzene (mCP), which lacks the coordinating pyridyl group in mCPy. The emission spectrum of the CuI:mCP film was identical to that of mCP ( $\lambda_{max} = 425$  nm), indicating that pyridine coordination is required for formation of the emissive species in the CuI:mCPy film.

CuI:mCPy films were used to fabricate four OLEDs [ITO/NPD (25 nm)/CuI:mCPy (20 nm)/BCP (40 nm)/LiF (1 nm)/Al (100 nm), where NPD =  $N,N'$ -bis(naphthalen-1-yl)- $N,N'$ -bis(phenyl)benzidine, BCP = bathocuproine] in which the molar ratios of the CuI:mCPy films were 0:1 (device 1), 1:4 (device 2), 1:6 (device 3), and 1:10 (device 4). Figure 2 shows EL spectra of the devices at 8 V. The emission from devices 2–4 was significantly different from that of device 1, indicating that the luminescence arises from a CuI:mCPy complex, consistent with the aforementioned PL study. EL solely from CuI:mCPy was observed in device 2 under all applied voltages. Devices 3 and 4, with higher mCPy concentrations, exhibited a very small emissive contribution from mCPy at high applied voltages (see Supporting Information). Among OLEDs 1–4, device 4 with the greatest amount of mCPy (CuI:mCPy = 1:10) showed the highest external quantum efficiency (EQE = 3.2%).

Two more devices were fabricated with a tris(8-hydroxyquinolino)aluminum ( $Alq_3$ ) electron transport layer (ETL). The structure was ITO/NPD (25 nm)/CuI:mCPy (1:5, 20 nm)/BCP ( $x$ )/ $Alq_3$  (30 nm)/LiF (1 nm)/Al (100 nm), where the

Table 2. Performance of Devices 1–6

device	$V_{on}$ (V) <sup>a</sup>	$L_{max}$ (cd/m <sup>2</sup> )	EQE <sub>max</sub> (%)	PE <sub>max</sub> (lm/W)	CE <sub>max</sub> (cd/A)
1	6.4	2500	0.54	0.28	0.86
2	3.6	8800	2.4	3.8	7.4
3	3.5	9900	3.0	4.9	9.7
4	3.7	9100	3.2	5.3	9.8
5	3.5	9100	3.9	10.3	11.7
6	3.6	9700	4.4	10.2	13.8

<sup>a</sup>  $V_{on}$  is the voltage required to reach a brightness of 1 cd/m<sup>2</sup>.

thickness of the BCP layer was either  $x = 10$  nm (device 5) or  $x = 0$  nm (device 6). The two devices had emission spectra similar to that of device 3, indicating that hole–electron combination occurs within the CuI:mCPy layer and that EL arises from a CuI:mCPy complex. As shown in Table 2, device 6 gave the highest EQE (4.4%), power efficiency (PE = 10.2 lm/W), and current efficiency (CE = 13.8 cd/A). Device 6 with  $Alq_3$  as the sole ETL gave a higher efficiency than devices containing BCP (i.e., 2–5), likely as a result of a better balance of charge injection and transport. Moreover, the increase in efficiency suggests that further improvement in performance can be achieved by optimizing the device configuration.

Our initial lifetime measurements on CuI:mCPy-based OLEDs are encouraging. In this study, we monitored the light output of device 6 under vacuum (150 mTorr) while driving the device at a current density of 20 mA/cm<sup>2</sup> (brightness = 2100 cd/m<sup>2</sup>). The half-life for the device under these conditions was 21 h, corresponding to 440 h at 100 cd/m<sup>2</sup>. While this is well below the lifetimes reported for optimized OLEDs, it is a factor of 5 longer than that for an analogous device with the CuI:mCPy emissive layer replaced with a 20 nm layer of Ir(ppy)<sub>3</sub>:mCPy [10 wt %, Ir(ppy)<sub>3</sub> = *fac*-tris(2-phenylpyridine)iridium]. When this Ir(ppy)<sub>3</sub>-based device was driven under the same conditions, a projected half-life of 75 h at 100 cd/m<sup>2</sup> was observed. This indicates that the CuI:mCPy emissive layer is quite stable and promising for OLED applications.

Previous work has shown that the three main products from reactions of CuI and pyridine, namely, [CuI(py)]<sub>∞</sub>, [CuI(py)<sub>2</sub>]<sub>2</sub>, and [CuI(py)<sub>4</sub>] (py = pyridine), show blue, green, and orange emission, respectively, in the solid state at rt.<sup>5a</sup> We prepared several related complexes to model the luminescent species in the codeposited CuI:mCPy film. [CuI(mCPy)]<sub>∞</sub> (model A) was synthesized via the reported method for [CuI(py)]<sub>∞</sub><sup>5a</sup> and characterized by elemental analysis and emission spectroscopy. The complex gave blue emission with  $\lambda_{max} \approx 480$  nm (Figure 3) and a PL quantum yield (PLQY) of 64% in the solid state at rt. The emission exhibited a slight red shift as  $T$  decreased to 77 K ( $\lambda_{max} = 486, 508$  nm). The PL lifetimes measured at 480 nm were found to be 3.0 and 16.8  $\mu$ s at rt and 77 K, respectively.

Another model complex, [CuI(mCPy)]<sub>4</sub>·3CH<sub>2</sub>Cl<sub>2</sub> (model B1), was synthesized by mixing CuI and mCPy in CH<sub>2</sub>Cl<sub>2</sub> and characterized by single crystal X-ray diffraction. The structure consists of Cu<sub>4</sub> tetrahedra with iodides capping all four faces and the mCPy pyridyl ligands at the apexes (Figure 3). This structure is similar to that of [CuI(py)]<sub>4</sub>.<sup>6b</sup> Model B1 gave a primary emission band at  $\sim 560$  nm with a decay lifetime of 2.1  $\mu$ s at rt. Exposure of crystalline B1 to vacuum resulted in loss of CH<sub>2</sub>Cl<sub>2</sub>, forming [CuI(mCPy)]<sub>4</sub> (model B2) with dominating emission at 620 nm and a decay lifetime of 7.3  $\mu$ s. Both B1 and B2 showed clear luminescent thermochromism with strong blue emission

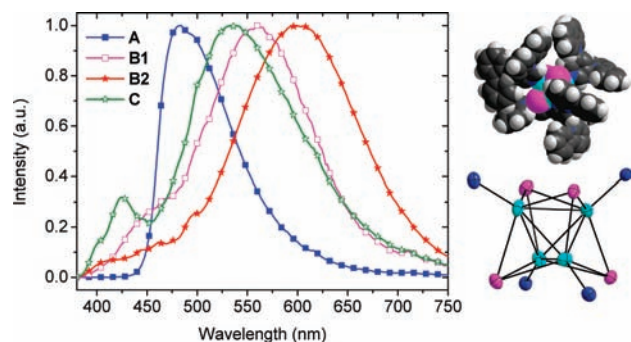


**Figure 3.** (left) PL spectra ( $\lambda_{\text{ex}} = 350 \text{ nm}$ ) of  $[\text{CuI}(\text{mCPy})]_{\infty}$  (model A), B1,  $[\text{CuI}(\text{mCPy})]_4$  (model B2), and ground CuI with mCPy (model C). (right top) Space-filling drawing of  $[\text{CuI}(\text{mCPy})]_4 \cdot 3\text{CH}_2\text{Cl}_2$  (model B1) from crystal coordinates. (right bottom) ORTEP structure (50%) of the  $\text{Cu}_4\text{I}_4$  core of B1 with only the coordinating N atoms of the mCPy ligands shown.

( $\lambda_{\text{max}} = 500 \text{ nm}$ ) at 77 K and decay lifetimes of  $\sim 30 \mu\text{s}$ , similar to many reported  $(\text{CuI})_4$  clusters.<sup>5a,8</sup> In contrast, the codeposited films showed identical spectra at 298 and 77 K.

It was found that an amorphous material (model C) prepared by simple grinding of CuI with mCPy in a 1:4 molar ratio gave emission centered at 530 nm with decay lifetimes of 4.0 (37%) and 11.0 (63%)  $\mu\text{s}$ , quite similar to our deposited films. No complex could be isolated on dissolution of model C, since it transformed to polymeric  $[\text{CuI}(\text{mCPy})]_{\infty}$  in  $\text{CH}_3\text{CN}$  and tetrameric  $[\text{CuI}(\text{mCPy})]_4$  in  $\text{CH}_2\text{Cl}_2$ . Moreover, grinding either  $[\text{CuI}(\text{mCPy})]_{\infty}$  or  $[\text{CuI}(\text{mCPy})]_4$  with or without mCPy gave a material having photophysical properties similar to those of the codeposited CuI:mCPy film, although the most efficient emission was observed with added mCPy.

To characterize the structure of the luminescent species in codeposited films, we used XAS. In order to generate sufficient material,  $\sim 2 \mu\text{m}$  CuI:mCPy films (ratio = 1:2.5) were deposited on five four-inch Si wafers and scraped off to give a 40 mg powdered sample (model D). The molar ratio was confirmed by elemental analysis. Model D showed photophysical properties identical to those of the codeposited films used for photophysical and EL studies. Details of sample preparation, characterization, data collection, and analysis for XAS are given in the Supporting Information. Investigation of the XANES pre-edge region confirmed the presence of only monovalent Cu in the sample. The XANES spectrum was compared with those of the known two-, three-, and four-coordinate model complexes  $[\text{Cu}(\text{xypz})_2(\text{BF}_4)_2]$  [ $\text{xypz} = \text{bis}(3,5\text{-dimethylpyrazoyl-}m\text{-xylene})$ ],  $[(\text{C}_6\text{H}_5)_4\text{P}]_2[\text{Cu}(\text{SC}_6\text{H}_5)_3]$ , and  $[\text{Cu}(\text{py})_4]\text{ClO}_4$ , respectively (Figure S12).<sup>9</sup> The intensity of the peak at  $\sim 8984.5 \text{ eV}$ , which is characteristic of  $1s \rightarrow 4p$  transitions in Cu(I) species, precluded the possibility of two-coordinate Cu(I) in the sample. The energy of the three-coordinate Cu(I) model complex closely matched that of the Cu(I) in the film. However, the energy of the  $1s \rightarrow 4p$  transition can decrease with  $\text{I}^-$  ligation because of greater electron-donating ability of  $\text{I}^-$  than of the N/S-based ligands of the model complexes, which results in a lower  $Z_{\text{eff}}$ . In addition, decreased antibonding of the halide orbitals with Cu(I) 4p orbitals in comparison with the N/S ligand reference complexes can also contribute to a shift to lower energy. Thus, the data are also consistent with the presence of a four-coordinate Cu(I) species in the CuI:mCPy film (model D).

The Fourier transform (FT) is shown in Figure 4, and the EXAFS fit parameters are given in Table 3. Table 3 also gives

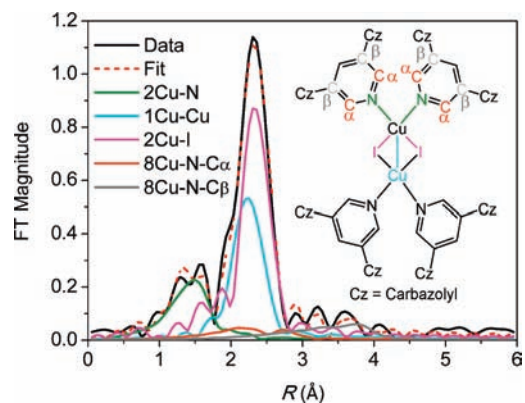


**Figure 4.** Non-phase-shift-corrected Fourier transform of codeposited CuI:mCPy film species (model D, CuI:mCPy = 1:2.5). Inset: chemical structure of  $[\text{CuI}(\text{mCPy})_2]_2$ . The phase shift in the first shell was  $\sim 0.4 \text{ \AA}$ . Data, fit, and deconvoluted waves are shown.

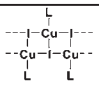
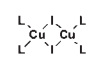
EXAFS fit parameters for polymeric model complex A and related parameters (derived from crystallographic coordinates) for model B1 and  $[\text{CuI}(\text{pyCN})_2]_2$ <sup>10</sup> (pyCN = 3-cyanopyridine) (model E) for comparison. The combination of one Cu–Cu and two Cu–I paths around  $2.6 \text{ \AA}$  gave the best fit to the data. The distance and  $\sigma^2$  parameter for the two paths were strongly correlated. On the other hand, a poor fit to the data was found when either of those paths was excluded or when any one of the two paths, in the absence of the other, was split into two. Other coordination numbers between 1 and 4 for Cu–Cu and Cu–I can be excluded on the basis of a poorer fit factor,  $F$ , and/or higher  $\sigma^2$ . A Cu–N path at  $2.02 \text{ \AA}$  was also necessary. A slight, albeit insignificant, improvement in the fit was observed using a two Cu–N rather than a one Cu–N path.

Analysis of the EXAFS and FT data enabled us to distinguish the major Cu(I) species present in the CuI:mCPy film. The data for model D and the  $[\text{CuI}(\text{mCPy})]_{\infty}$  polymer (Figures S13–S15) showed major differences, confirming that the CuI:mCPy film and polymer consist of different species. A complex related to model B1 could also be eliminated as a possibility by comparison of the Cu–Cu and Cu–I coordination numbers in Table 3. The structural parameters for model D closely match those reported in the literature for model E.<sup>10</sup> Thus, on the basis of both the luminescence spectra and XAS studies, the emitting species in CuI:mCPy thin films is most likely the dimeric complex  $[\text{CuI}(\text{mCPy})_2]_2$  (illustrated in the Figure 4 inset), with small variable amounts of  $[\text{CuI}(\text{mCPy})]_{\infty}$  in low enough concentration that it does not contribute significantly to the XAS.

Codeposition of mCPy with CuBr and CuCl was also examined. Both CuBr and CuCl reacted with mCPy to form luminescent films. However, neither halide material showed a luminescence efficiency comparable to the CuI-based materials. Films made using CuBr displayed an emission peak at 550 nm ( $\tau = 6.7 \mu\text{s}$ ) with a maximum PLQY of 37%. The CuCl-based film had a red-shifted emission peak at 570 nm ( $\tau = 3.1 \mu\text{s}$ ) and a lower PLQY of 14%. The red-shifted emission spectra and decreased PLQY are consistent with the low ligand-field strengths of the Br and Cl anions and the expected reduction in spin–orbit coupling for the lower- $Z$  halogens.

We also examined thin films prepared by codeposition of CuI and the common OLED materials 1,3,5-tris( $N$ -phenylbenzimidazole-2-yl)benzene (TPBi) and 2-(4-biphenyl)-5-(4-*tert*-butylphenyl)-1,3,4-oxadiazole (PBD). Emission from both the

**Table 3. EXAFS Least-Squares Fitting Results for  $k = 2-13.4 \text{ \AA}^{-1}$  for Codeposited CuI:mCPy Film Species (Model D) and Key Parameters for Model Complexes  $[\text{CuI}(\text{mCPy})]_{\infty}$  (Model A),  $[\text{CuI}(\text{mCPy})]_4 \cdot 3\text{CH}_2\text{Cl}_2$  (Model B1), and  $[\text{CuI}(\text{pyCN})_2]_2$  (Model E)**

Model	Path	Cu-Cu	Cu-I	Cu-N	Cu-N-C $_{\alpha}$	Cu-N-C $_{\beta}$
<b>D<sup>a</sup></b> film	Coord. $R(\text{\AA})^b$ $\sigma^2(\text{\AA}^2)^c$	1 2.60 755	2 2.63 570	2 2.02 1108	8 3.23 663	8 4.34 756
<b>A<sup>d</sup></b> (CuIL) $_{\infty}$	 Coord. $R(\text{\AA})$	2	3	1		
<b>B1<sup>e</sup></b> (CuIL) $_4$	See Figure 3 right bottom Coord. $R(\text{\AA})$	3	3	1		
<b>E<sup>e</sup></b> (CuIL $_2$ ) $_2$	 Coord. $R(\text{\AA})$	1	2	2		

<sup>a</sup>  $\Delta E_0(\text{eV}) = -13.68$  for the EXAFS fit of **D**, while the goodness of fit ( $F_{\text{normalized}}$ , defined by  $\Sigma[(\chi_{\text{obsd}} - \chi_{\text{calcd}})^2 k^6] / \Sigma[(\chi_{\text{obsd}})^2 k^6]^{0.5}$ ) was 0.117. <sup>b</sup> The estimated standard deviation of  $R$  for each fit was  $\pm 0.02 \text{ \AA}$ . <sup>c</sup> The  $\sigma^2$  values have been multiplied by  $10^5$ . <sup>d</sup> The EXAFS fit for **A** is shown in the Supporting Information. <sup>e</sup> Parameters for **B1** and **E** were taken from their respective crystal structures.

TPBi- and PBD-based films gave substantial components for the organic materials themselves as well as a CuI complex (see Supporting Information) and only moderate PLQYs ( $\sim 17$  and  $14\%$ , respectively). The low efficiency and ligand contamination of the spectra are likely due to the fact that both TPBi and PBD are poor ligands for Cu, leading to incomplete formation of the emissive Cu(I) complex.

In summary, we have demonstrated that CuI coordination complexes can be formed in situ by codeposition of CuI and ligand, leading to efficient OLEDs containing Cu(I) complexes. The ligand material in this case serves a dual role as both a ligand for forming the emissive complex and as a host matrix for the formed emitter. While complex formation occurs for a number of materials, care must be taken in the design of the organic material to ensure that it is a good ligand for Cu coordination. This new approach may be easily extended to other ligands to generate functional layers for use in organic optoelectronic devices.

## ■ ASSOCIATED CONTENT

**S Supporting Information.** Experimental details; PL and EL data; decay lifetimes; comparison of XANES data; EXAFS fit; and crystallographic data (CIF). This material is available free of charge via the Internet at <http://pubs.acs.org>.

## ■ AUTHOR INFORMATION

**Corresponding Author**  
met@usc.edu

## ■ ACKNOWLEDGMENT

We gratefully acknowledge financial support of this work from Universal Display Corporation and the Center for Energy Nanoscience, an Energy Frontier Research Center funded by the U.S. Department of Energy, Office of Science, Office of Basic Energy Sciences (DE-SC0001011). Portions of this research

were carried out at the Stanford Synchrotron Radiation Light-source (SSRL). The SSRL Structural Molecular Biology Program is supported by the DOE Office of Biological and Environmental Research and by the National Institutes of Health (NIH), National Center for Research Resources (NCRR), Biomedical Technology Program (P41RR001209). This study was supported in part by the NCRR (Grant 5 P41 RR001209), a component of the NIH.

## ■ REFERENCES

- (1) (a) Baldo, M. A.; Lamansky, S.; Burrows, P. E.; Thompson, M. E.; Forrest, S. R. *Appl. Phys. Lett.* **1999**, *75*, 4. (b) Lamansky, S.; Djurovich, P. I.; Murphy, D.; Abdel-Razzaq, F.; Lee, H. E.; Adachi, C.; Burrows, P. E.; Forrest, S. R.; Thompson, M. E. *J. Am. Chem. Soc.* **2001**, *123*, 4304. (c) Djurovich, P. I.; Thompson, M. E. In *Highly Efficient OLEDs with Phosphorescent Materials*; Yersin, H., Ed.; Wiley-VCH: Berlin, 2007; Chapter 3, pp 131–161. (d) Thompson, M. E.; Djurovich, P. I.; Barlow, S.; Marder, S. R. In *Comprehensive Organometallic Chemistry*; O'Hare, D., Ed.; Elsevier: Oxford, 2007; Vol. 12, pp 101–194.
- (2) (a) Ford, P. C.; Cariati, E.; Bourassa, J. *Chem. Rev.* **1999**, *99*, 3625. (b) Armaroli, N.; Accorsi, G.; Cardinali, F.; Listorti, A. *Top. Curr. Chem.* **2007**, *280*, 69. (c) Scaltrito, D. V.; Thompson, D. W.; O'Callaghan, J. A.; Meyer, G. J. *Coord. Chem. Rev.* **2000**, *208*, 243. (d) McMillin, D. R.; McNett, K. M. *Chem. Rev.* **1998**, *98*, 1201.
- (3) Manbeck, G. F.; Brennessel, W. W.; Evans, C. M.; Eisenberg, R. *Inorg. Chem.* **2010**, *49*, 2834.
- (4) (a) Zhang, Q. S.; Zhou, Q. G.; Cheng, Y. X.; Wang, L. X.; Ma, D. G.; Jing, X. B.; Wang, F. S. *Adv. Mater.* **2004**, *16*, 432. (b) Che, G. B.; Su, Z. S.; Li, W. L.; Chu, B.; Li, M. T.; Hu, Z. Z.; Zhang, Z. Q. *Appl. Phys. Lett.* **2006**, *89*, No. 103511. (c) Su, Z. S.; Che, G. B.; Li, W. L.; Su, W. M.; Li, M. T.; Chu, B.; Li, B.; Zhang, Z. Q.; Hu, Z. Z. *Appl. Phys. Lett.* **2006**, *88*, No. 213508. (d) Tsuboyama, A.; Kuge, K.; Furugori, M.; Okada, S.; Hoshino, M.; Ueno, K. *Inorg. Chem.* **2007**, *46*, 1992. (e) Deaton, J. C.; Switalski, S. C.; Kondakov, D. Y.; Young, R. H.; Pawlik, T. D.; Giesen, D. J.; Harkins, S. B.; Miller, A. J. M.; Mickenberg, S. F.; Peters, J. C. *J. Am. Chem. Soc.* **2010**, *132*, 9499. (f) Armaroli, N.; Accorsi, G.; Holler, M.; Moudam, O.; Nierengarten, J. F.; Zhou, Z.; Wegh, R. T.; Welter, R. *Adv. Mater.* **2006**, *18*, 1313.
- (5) (a) Kyle, K. R.; Ryu, C. K.; Dibenedetto, J. A.; Ford, P. C. *J. Am. Chem. Soc.* **1991**, *113*, 2954. (b) Kim, T. H.; Shin, Y. W.; Jung, J. H.; Kim, J. S.; Kim, J. *Angew. Chem., Int. Ed.* **2008**, *47*, 685. (c) Araki, H.; Tsuge, K.; Sasaki, Y.; Ishizaka, S.; Kitamura, N. *Inorg. Chem.* **2005**, *44*, 9667.
- (6) (a) Dyason, J. C.; Healy, P. C.; Pakawatchai, C.; Patrick, V. A.; White, A. H. *Inorg. Chem.* **1985**, *24*, 1957. (b) Raston, C. L.; White, A. H. *J. Chem. Soc., Dalton Trans.* **1976**, 2153. Rath, N. P.; Maxwell, J. L.; Holt, E. M. *J. Chem. Soc., Dalton Trans.* **1986**, 2449. (d) Eitel, E.; Oelkrug, D.; Hiller, W.; Strahle, J. Z. *Naturforsch., B* **1980**, *35*, 1247.
- (7) De Angelis, F.; Fantacci, S.; Sgamellotti, A.; Cariati, E.; Ugo, R.; Ford, P. C. *Inorg. Chem.* **2006**, *45*, 10576.
- (8) (a) Perruchas, S.; Le Goff, X. F.; Maron, S.; Maurin, I.; Guillen, F.; Garcia, A.; Gacoin, T.; Boilot, J. P. *J. Am. Chem. Soc.* **2010**, *132*, 10967. (b) Tard, C.; Perruchas, S.; Maron, S.; Le Goff, X. F.; Guillen, F.; Garcia, A.; Vigneron, J.; Etcheberry, A.; Gacoin, T.; Boilot, J. P. *Chem. Mater.* **2008**, *20*, 7010.
- (9) Kau, L. S.; Spirasolomon, D. J.; Pennerhahn, J. E.; Hodgson, K. O.; Solomon, E. I. *J. Am. Chem. Soc.* **1987**, *109*, 6433–6442.
- (10) Huang, X. C.; Ng, S. W. *Acta Crystallogr.* **2004**, *60*, m1055.